www.MaterialsViews.com

Bionanotechnology

Trajectory-Based Co-Localization Measures for Nanoparticle-Cell Interaction Studies

Juan A. Varela, Christoffer Åberg, Jeremy C. Simpson, and Kenneth A. Dawson**

1. Introduction

A large number of studies in recent years have focused on understanding the interactions between nano-scale objects and biological systems.[1–3] Of primary focus has been the study of uptake and, ultimately, fate of nanoparticles (NPs) when encountering cells. While no definitive molecular description of their internalization mechanism has emerged to date,[4] a dominant role of endo/lysosomal trafficking pathways after uptake is relatively well established.[4–6] Nevertheless, much remains to be explored regarding NP intracellular localization, notably a deeper understanding of the specific intracellular compartments through which they pass. Central to this is the ability to use light microscopy approaches to make a reliable quantification of NP/organelle or NP/fluorescent label co-localization.

One of the main advantages of fluorescence light microscopy is its capability of imaging live samples. As long as a specific fluorescent label is available and the microscope has adequate sensitivity and speed, fluorescence light microscopy is one of the most reliable methods for understanding living processes. In particular, time-lapse experiments facilitate the study of dynamic cellular events, ranging from sub-millisecond time-intervals to hours or even days. Analysis of living cells potentially produces more direct – and therefore more reliable – data for understanding living processes in real time. Individual cells can be imaged either continuously, or at defined intervals, rather than sampling at one specific time point, as is typically the case in flow cytometry. In addition, fluorescence imaging provides a richer depth of single cell data, whereas methods such as colorimetric assays only provide mean results from a population. Furthermore, the availability of a wide range of fluorescent probes allows the visualization and quantification of the temporal and spatial dynamics of molecules and organelles, and study of physiological activities within living cells in real time, avoiding fixation artifacts.

A prevalent tool for the analysis of biological microscopy images is the evaluation of co-localization between signals (or colors) detected in two different channels. The main methods to quantify co-localization include the evaluation of co-occurrence of signal in both channels, measurement of the correlation of the signals in both channels, and object-based co-localization relying on the co-occurrence of segmented structures. Early quantitative analyses of co-localization in microscopy images.[7] were based on a well-established measurement of the linear correlation between variables, namely the Pearson's correlation coefficient. This coefficient is symmetric in the two signals, that is, the co-localization of the first signal with the second is the same as the co-localization of the second with the first. This feature may be deemed undesirable, however, for example in the case where one species is always found in close proximity to a second species, but where the second species may also be found alone. This observation may be biologically important, but the symmetry of the Pearson's correlation coefficient obscures this information.

An alternative to the Pearson's correlation coefficient is the Manders' overlap coefficient, another widely used method to evaluate co-localization[8] that indicates the proportion of the signal in a channel that coincides with the other channel. In contrast to the Pearson correlation coefficient the Manders overlap coefficient is asymmetric in the two channels. However, this metric suffers from the problem that it is insensitive to intensity correlation. We have recently proposed a new co-localization measure, weighting the co-occurrence of the signal with the intensity information in each pixel,[9] thereby minimizing some of the weaknesses associated with the Pearson and Manders methods. In general, each of these co-localization coefficients can be useful to quantify the overall co-localization between proteins in cells,[10] but in the case of organelles or other distinct punctate structures (e.g. NPs), these can be directly identified and a more accurate co-localization value achieved using object-based compared to pixel-based methods. Additionally, if live cells are imaged in a time-lapse fashion, the analysis of the images can be enriched by taking account of the temporal evolution of segmented structures. The detection and tracking of single molecules, structures or entire organelles provide information about

Dr. J. A. Varela, Dr. C. Åberg, Prof. K. A. Dawson
Centre for BioNano Interactions
School of Chemistry and Chemical Biology – University College Dublin
Belfield, Dublin 4, Ireland
E-mail: juan.varela@u-bordeaux.fr; kenneth.a.dawson@cbni.ucd.ie

Prof. J. C. Simpson
School of Biology and Environmental Science and Conway Institute of Biomolecular and Biomedical Research – University College Dublin
Belfield, Dublin 4, Ireland

DOI: 10.1002/smll.201401849

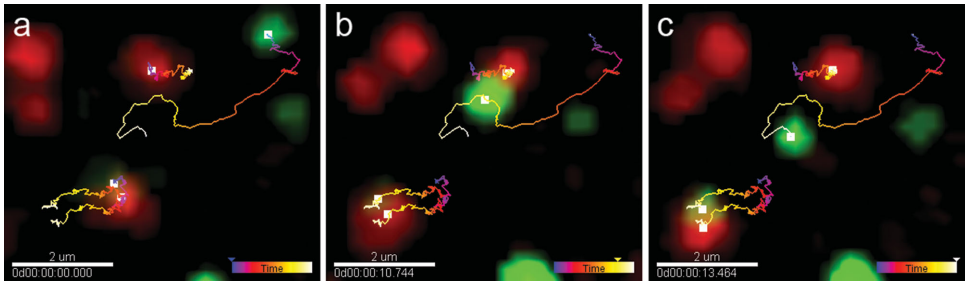

Figure 1. Persistent and spurious co-localization in two dimensions. a–c) Snapshots at various time-points taken from a live cell movie corresponding to an A549 cell labeled with LysoTracker Red and incubated with 100 nm PS-COOH green fluorescent nanoparticles (scale-bar 1.5 μm; full movie provided in the Supporting Information). Reconstructed trajectories illustrate how single time-points are not enough to evaluate co-localization.

the dynamics of co-localization events, while simultaneously reducing the spurious detection of co-localization given by a purely transient proximity between objects.

Over the last few years, single particle tracking (SPT) has become a fundamental tool to study the dynamics of cellular organelles and even single molecules.[11–17] SPT has also become valuable to the bio-nano field, with applications including the characterization of dispersions of synthetic NPs in biologically relevant environments,[18] the study of the intracellular transport of NPs,[19] and using NPs as probes to track or sense biological events.[20–22] There are several studies in which the advantages of using trajectories of single molecules to study molecular interactions have been described, for example a study of E-cadherin molecules diffusing in the cellular plasma membrane.[23] At the intracellular trafficking level, the internalization and fate of polymeric gene complexes have also been studied with SPT techniques, evaluating co-localization between these complexes and cellular organelles tagged with EGFP using time information from reconstructed trajectories.[24] The study of dynamic events in cells still needs to be further developed using automated segmentation and trajectory analysis, in order to extract more significant information from microscopy images.

In this concept paper we highlight the importance of using temporal information for evaluating co-localization between two objects. This is particularly relevant to studies on NPs, because their ease of detection facilitates the procedure, but it could equally well be applied to other punctuate structures found in cells. We discuss the disadvantages of static co-localization measures, and illustrate how including temporal information resolves these. We conclude with a case-study using a trajectory-based co-localization measure.

2. Results and Discussion

As an illustration of the importance of including temporal information, we observed the behaviour of 100 nm carboxylated polystyrene (PS-COOH) NPs and lysosomes in a living A549 lung carcinoma cell (**Figure 1**, the full movie is provided in Movie S1, Supporting Information). For this experiment, the cell was previously incubated with LysoTracker Red (0.75 μM for 60 min), subsequently exposed to the NPs (100 μg mL^{-1} for 10 min), and then imaged in two dimensions on a spinning disk confocal microscope (see Experimental Section for details). Figure 1 shows two sets of intracellular trajectories, in which the first example (lower objects) has a persistent co-localization, enduring throughout the 13.5 s of the imaging. In the second example (upper objects) the co-localization is instead transient, the two objects initially being separated, coming together for approximately 2 s and then separating again. Naturally, if a single image was taken at a time when both trajectories overlap (Figure 1b), both events would be counted as co-localized, thus over-estimating the actual co-localization.

To illustrate quantitatively the effect of not including temporal information, we can calculate the change in co-localization according to two paradigms of motion, namely active and diffusive (Brownian) motion. While the detailed type of intracellular motion will not necessarily conform to either of these paradigms, they do give a sense of scale. To this end, consider two objects initially overlapping in an image, but not actually co-localized. If a snapshot was taken at the initial time, the two objects would appear co-localized, but with time the objects move away from each other and the (apparent) co-localization decreases. When the objects are separated by more than 250 nm from each other (the order of magnitude of the distance being set by half the wavelength of the light, as dictated by the diffraction limit), they will no longer appear co-localized. If the motion is active, the time it takes for the (apparent) co-localization to disappear depends upon the velocities involved (both the relative speeds and the angle of the two trajectories). **Figure 2**a shows the apparent co-localization as a function of observation time for several different speeds, ranging from 1.2 μm s^{-1} to 25 μm s^{-1}. The particular speeds were taken from a system where the speeds have been measured in detail, namely for peroxisome movement in cultured *Drosophila* S2 cells,[25] and correspond to the lower peak in the speed distribution and twice the maximum speed (emulating two objects moving in opposite direction), respectively. In the latter case, only 0.01 s would be enough to differentiate a spurious co-localization from an actual one, while for the slower motion, as shown in Figure 2b, just over 0.2 s are needed.

For diffusive (Brownian) motion on the other hand, the apparent co-localization of two objects initially in close proximity to one another is stochastic. Furthermore, in this scenario the co-localization depends on how quickly they diffuse away from each other; namely their diffusion coefficients. Figure 2b shows the (apparent) co-localization for symmetric

www.MaterialsViews.com

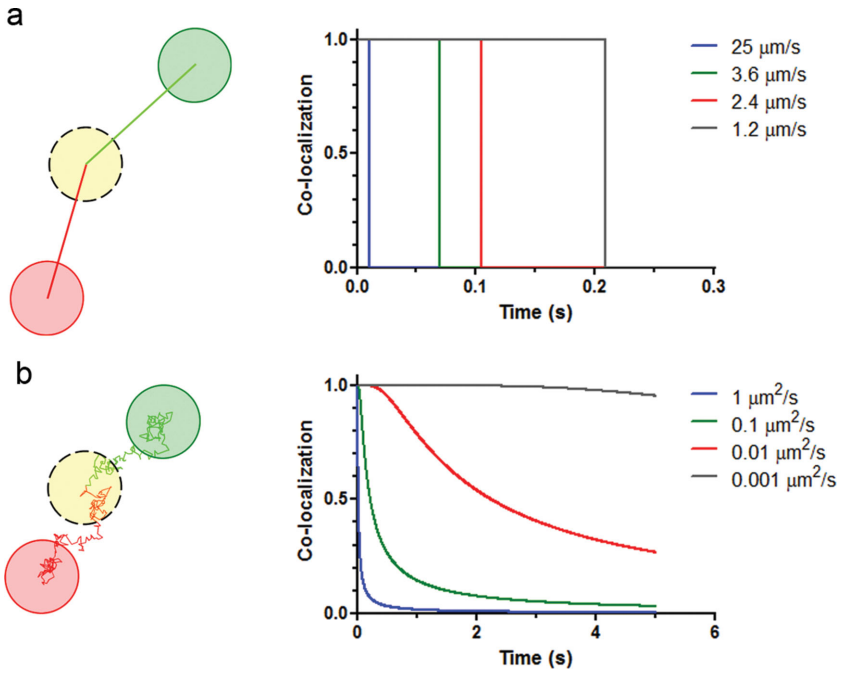

Figure 2. Quantitative estimate of spurious co-localization in two dimensions for active and diffusive (Brownian) motion. a) Schematic of two objects, initially in close proximity to one another, moving away from each other by active motion, together with corresponding theoretical co-localization as a function of observation time for several different speeds. The time it takes for the objects to depart depends on both the relative speed, as well as the angle of the trajectories. b) Schematic of two objects, initially in close proximity, diffusing away from each other, and the theoretical co-localization as a function of observation time for several different diffusion coefficients.

diffusion (see Supporting Information for details), utilizing diffusion coefficients ranging from 0.001 $\mu m^2\ s^{-1}$ to 1 $\mu m^2\ s^{-1}$, where the lower value would be analogous to endosomes in cells moving less than the typical detection noise (as can be estimated from the detection of NPs stuck to the glass coverslip). Here we observe a decrease in the co-localization, reflecting the need for temporal information in order to generate adequate co-localization measurements. For the slow moving objects, temporal tracking should be performed for at least 5 to 10 s to minimize the effect of spurious co-localization, while for the faster moving objects, tracking over 1 s would be enough to discard spurious co-localization measurements. While estimates such as those shown in Figure 2 are somewhat idealized (for example not including the initial separation distance between the objects), they do indicate the scale of the problem – as well as the length of time needed to follow the objects if accurate measurements are to be made.

Further information about co-localization events is obtained if the imaging is performed in three dimensions. Although the study of adherent cell cultures is often simplified to two-dimensional approaches for many practical purposes, the three-dimensional nature of cells often needs to be taken into account to understand cellular processes. If the motion of organelles is analyzed in two dimensions, measured speeds are going to be lower than real speeds, as the projected two-dimensional travelled distance is smaller than the three-dimensional one. Another limitation of two-dimensional particle tracking has been shown by Gratton and colleagues,[26] in which deformation studies of the cytoskeleton reveal that planar stresses produce strain in three dimensions, and therefore two-dimensional particle tracking fails to give accurate results.

As a proof of concept, we now present a temporal co-localization analysis, in three dimensions, showing the intracellular transport of fluorescently-labeled polystyrene NPs at a single NP level in live cells. This analysis method is likely to be suitable for many other types of fluorescent NPs, as long as they are sufficiently bright to be identified individually, and their fluorescence dispersion is reasonably homogeneous to allow the accurate quantification of NPs when examining clusters inside organelles smaller than the optical resolution limit. While a temporal co-localization analysis on a similar system has been performed previously,[24] this is to our knowledge the first time such an analysis has been performed in three dimensions. As a system, we analyzed the intracellular transport of 100 nm PS-COOH NPs in living A549 lung carcinoma cells, previously labeled with LysoTracker Red (cf. Figure 1). Cells were exposed to a concentrated NP dispersion (100 µg mL^{-1}) for 10 min ("pulse"), followed by careful Phosphate Buffered Saline (PBS) washes and addition of fresh growth medium. The cells were then observed ("chased") in a spinning disk confocal microscope at various times after NP exposure (see Experimental Section for details). In order to sample the time-course of NP trafficking within the cells, we selected a range of time-points for image acquisition and analysis, specifically 20 min, 45 min, 2 h, and 3 h after the 10 min NP pulse. Longer times were not considered due to a decrease in the LysoTracker label quality. This ("pulse-chase") experiment allowed us to follow a fixed population of NPs as they transit the cell and make their way through the endo-/lysosomal membrane system.

At each time-point, 25 consecutive three-dimensional images ("z-stacks") were acquired in order to track NPs and lysosomes. The acquisition was limited to these 25 three-dimensional stacks in order to avoid high degrees of photobleaching and subsequent photodamage to the cell. Future studies may explore the use of near infra-red probes,[27–30] which show increased photoresistance, in turn further minimizing damage to the cell (or tissue).

These images were first analysed according to well-established co-localization methods (Pearson and Manders), which in essence cannot (in their traditional utilization) use the information stemming from the high resolution temporal component. **Figure 3**e shows the co-localization between NPs and lysosomes obtained according to these measures (using the temporal information at each time-point solely to calculate deviation). While a clear trend of increased co-localization with time is observed for all

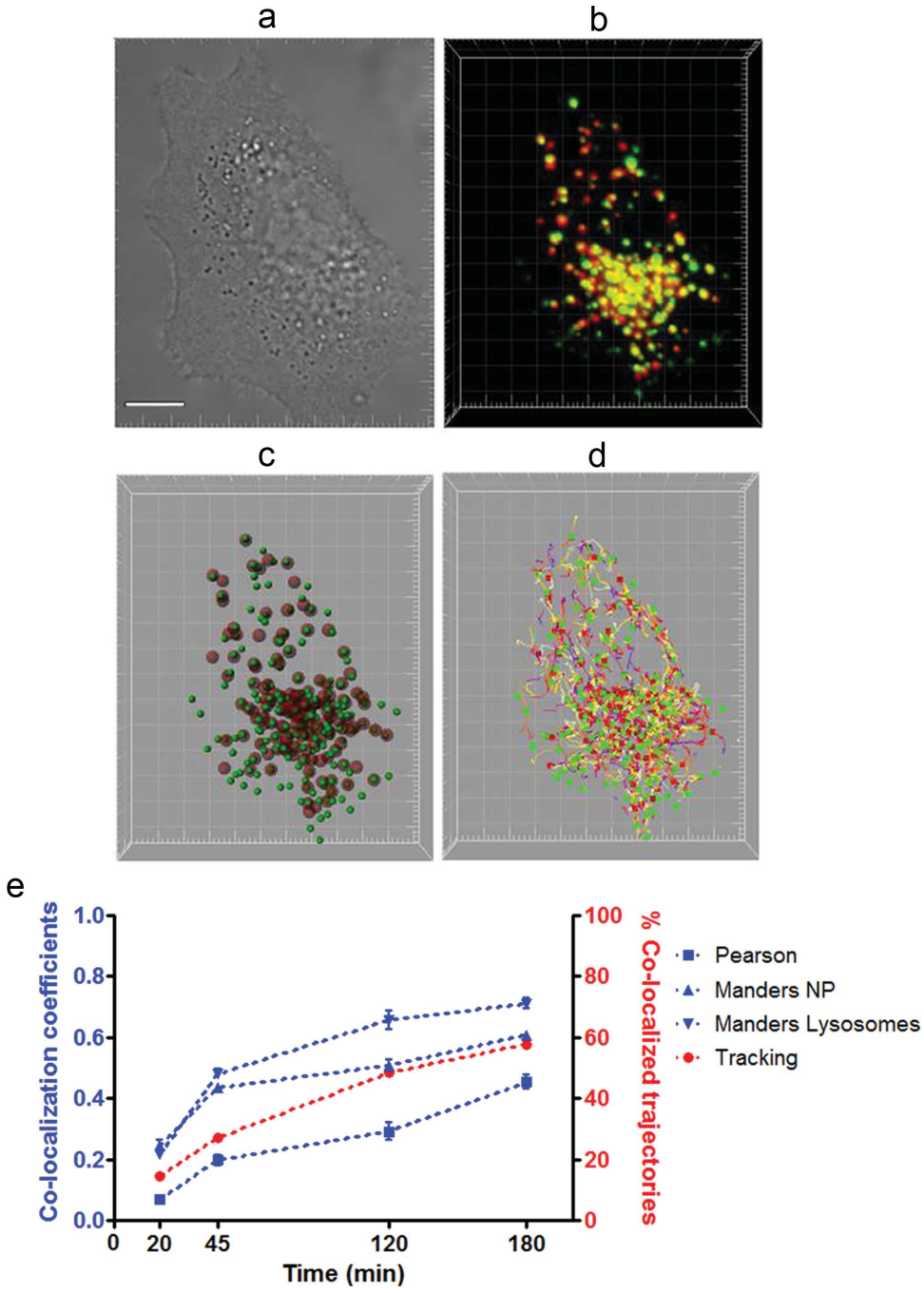

Figure 3. Three-dimensional tracking of nanoparticles in cells. a–d) Images corresponding to an A549 cell labeled with LysoTracker Red, 180 min after a 10 min exposure to 100 μg mL^{-1} of 100 nm PS-COOH nanoparticles. a) Bright field image (scale-bar 10 μm). b) Maximum intensity projection of the confocal three-dimensional fluorescence image. c) The lysosomes (red spots) and nanoparticles (green spots) were automatically identified and d) their trajectories subsequently determined. e) Co-localization between nanoparticles and lysosomes according to different measures. The plots with blue lines show Pearson, "Manders NP" and "Manders Lysosomes" co-localization coefficients of nanoparticles and lysosomes. Error bars correspond to standard deviation between the calculated coefficients for each of the 25 three-dimensional images. The red line shows a co-localization analysis based on the mean value of the LysoTracker Red signal throughout each nanoparticle trajectory, as described in the main text.

measures, there is nevertheless a wide spread in the actual values.

We next performed a temporal co-localization analysis, by using the trajectories of the NPs to assess the co-localization with lysosomes over time. For this purpose we took advantage of image segmentation to identify single NPs and cellular organelles from the images. Following image acquisition, the signals in both channels were analyzed with commercial software (Imaris, Bitplane Inc.). The bright spots corresponding to NPs or lysosomes were automatically identified for all frames, and subsequently linked in order to obtain the trajectories (Figure 3a–d and example movie provided in the

Movie S2, Supporting Information). Using the identified NPs as reference, we measured the levels of LysoTracker Red signal within a sphere of radius 0.5 μm centered on the position of each identified NP along the entire track. A threshold to determine whether there was a lysosome or not at a given position was assigned based upon the LysoTracker Red signal corresponding to an automated detection of lysosomes. If the average signal of LysoTracker Red along the trajectory was above the assigned threshold, then the detected NP spot was considered as co-localized with a lysosome. Subsequently, the intensity of each identified NP was used to weight the co-localization value in order to calculate the percentage of NPs that were inside lysosomes. This was done in a such a way that the final co-localization values shown are the proportion of intensity of co-localized NP with respect to the total NP intensity. This analysis revealed that this method produces co-localization data following a similar trend to the established co-localization measures (Figure 3e), but importantly the actual co-localization values were different from the other metrics, as a result of the conceptual differences by which they were determined.

Finally, it should be noted that the bottleneck in the co-localization analysis workflow presented here is not the co-localization detection itself, but rather the segmentation of structures and subsequent trajectory reconstruction. Software packages are constantly improving in this respect, but it still currently takes tens of minutes to analyze a three-dimensional movie, such as those presented in this study. Tracking performance can be further improved by using wavelet decomposition methods instead of fitting Gaussians,[31] or running code through graphics processing units (GPUs) instead of the central processing unit (CPU).[32] In the future, it should be expected that this analysis could be performed in near real time.

3. Conclusions

With this case study we have shown that SPT of fluorescently labeled NPs imaged in a confocal spinning disk microscope can provide valuable information to understand the intracellular transport of NPs. Following object detection, the analysis of the trajectories allowed us to quantify the co-localization of single NPs with lysosomes with greater accuracy, analyzing the entire cell in three dimensions.

From a broader perspective, our case study and this concept paper in general, illustrates the potential of using time resolution and object-based analysis in biological microscopy, and how it can be applied to improve the certainty of intracellular events, for NP-cell studies and beyond. As live-cell imaging techniques further improve, future studies may utilize increased sampling rates and decreased cell illumination levels, aiming to have a more comprehensive and quantitative picture of the intracellular transport of NPs in living cells.

4. Experimental Section

A549 cells were cultured at 37 °C in 5% CO_2 in minimum essential medium (MEM, with additional L-glutamine) supplemented with 10% Fetal Calf Serum (FCS, Gibco), 1% penicillin/streptomycin (Invitrogen Corp.), and 1% MEM non-essential amino acids (HyClone). Cells were subcultured 1:3 every second day by incubating them in 0.25% trypsin (Gibco) when they were confluent and resuspending cells in growth medium. Regular mycoplasma tests were carried out, using the mycoAlert kit (Lonza Inc. Allendale, NJ), showing that the cells were mycoplasma free.

For spinning disk confocal microscopy, 1.3×10^5 cells were seeded onto 35 mm MatTek dishes and incubated for 24 h before carrying out the experiment. Live cells were stained with LysoTracker Red dye (Molecular Probes) at 0.75 μM for 1 h in complete MEM at 37 °C and washed away before taking the cells to the microscope or adding the NPs.

Yellow-green carboxylated polystyrene NPs (FluoSpheres) with mean diameter of 100 nm were purchased from Molecular Probes and used without further chemical modification. Size and ζ-potential were determined using a Malvern Zetasizer Nano Series. Polystyrene NPs were diluted to 50 μg mL^{-1} in PBS or 250 μg mL^{-1} in complete growth medium before measurement. Measurements were conducted at pH 7.0 and 25 °C. Results are presented in Table S1, Supporting Information.

For live cell imaging experiments with NPs, cells were stained with LysoTracker Red as described above and were subsequently incubated with a concentrated NP dispersion (100 μg mL^{-1}) prepared in complete growth medium at 37 °C. Cells were then incubated with NPs for 10 min, after which the medium was removed and samples were washed 5 times with 1 mL PBS at 37 °C. Fresh medium (also at 37 °C) was then added to the cells, and imaging was performed in a live cell chamber, at 37 °C in a 5% CO_2 and 60% humidity atmosphere.

Dual color visualization of cell organelles or NPs, was performed on a spinning-disk confocal microscopy system consisting of a CSU10 spinning disk unit (Yokogawa Electric corporation) and an iXon EMCCD camera (Andor), mounted on an IX81 inverted microscope (Olympus) with climate control chamber. NPs were excited with a 488 nm laser line, and LysoTracker Red was excited using a 561 nm laser line. A 60 × 1.35 NA Olympus UPlanSAPO oil immersion objective was used. Images were acquired using Andor iQ software. Three dimensional images were acquired at about one stack per second, while two dimensional movies were acquired at 10 frames per second. Object identification and tracking were performed using Imaris (Bitplane AG, Zurich). NPs and lysosomes were identified as 'spots' based upon the fluorescence of the corresponding channels, and tracking was performed using Imaris autoregressive motion algorithm, allowing a maximum step of 1 μm without gaps.

Supporting Information

Supporting Information is available from the Wiley Online Library or from the author.

Acknowledgements

This work was supported by the EU Sixth Framework Programme project S.I.G.H.T (IST-2005–033700), the EU Seventh Framework

Programme project NanoTransKinetics (NMP4-2010-EU-US-266737), a Science Foundation Ireland grant (09/RFP/MTR2425) and the Irish Research Council for Science, Engineering and Technology (C.Å.). The J.C.S. lab is supported by a Principal Investigator award (09/IN.1/B2604) from Science Foundation Ireland.

[1] G. Oberdörster, E. Oberdörster, J. Oberdörster, *Environ. Health Perspect.* **2005**, *113*, 823.
[2] A. E. Nel, L. Mädler, D. Velegol, T. Xia, E. M. V Hoek, P. Somasundaran, F. Klaessig, V. Castranova, M. Thompson, *Nat. Mater.* **2009**, *8*, 543.
[3] M. P. Monopoli, C. Åberg, A. Salvati, K. A. Dawson, *Nat. Nanotechnol.* **2012**, *7*, 779.
[4] T.-G. Iversen, T. Skotland, K. Sandvig, *Nano Today* **2011**, *6*, 176.
[5] J. Rejman, V. Oberle, I. S. Zuhorn, D. Hoekstra, *Biochem. J.* **2004**, *377*, 159.
[6] T. dos Santos, J. Varela, I. Lynch, A. Salvati, K. A. Dawson, *PLoS One* **2011**, *6*, e24438.
[7] E. M. M. Manders, J. Stap, G. J. Brakenhoff, R. van Driel, J. A. Aten, *J. Cell Sci.* **1992**, *103*, 857.
[8] E. M. M. Manders, F. J. Verbeek, J. A. Aten, *J. Microsc.* **1993**, *169*, 375.
[9] V. R. Singan, T. R. Jones, K. M. Curran, J. C. Simpson, *BMC Bioinformatics* **2011**, *12*, 407.
[10] S. V Costes, D. Daelemans, E. H. Cho, Z. Dobbin, G. Pavlakis, S. Lockett, *Biophys. J.* **2004**, *86*, 3993.
[11] D. Sage, F. R. Neumann, F. Hediger, S. M. Gasser, M. Unser, *IEEE Trans. Image Process.* **2005**, *14*, 1372.
[12] D. Li, J. Xiong, A. Qu, T. Xu, *Biophys. J.* **2004**, *87*, 1991.
[13] V. Levi, A. S. Serpinskaya, E. Gratton, V. Gelfand, *Biophys. J.* **2006**, *90*, 318.
[14] S. Manley, J. M. Gillette, G. H. Patterson, H. Shroff, H. F. Hess, E. Betzig, J. Lippincott-Schwartz, *Nat. Methods* **2008**, *5*, 155.
[15] A. Kuzmenko, S. Tankov, B. P. English, I. Tarassov, T. Tenson, P. Kamenski, J. Elf, V. Hauryliuk, *Sci. Rep.* **2011**, *1*, 195.
[16] G. I. Mashanov, J. E. Molloy, *Biophys. J.* **2007**, *92*, 2199.
[17] L. Groc, M. Heine, S. L. Cousins, F. A. Stephenson, B. Lounis, L. Cognet, D. Choquet, *Proc. Natl. Acad. Sci. USA* **2006**, *103*, 18769.
[18] K. Braeckmans, K. Buyens, W. Bouquet, C. Vervaet, P. Joye, F. De Vos, L. Plawinski, L. Doeuvre, E. Angles-Cano, N. N. Sanders, J. Demeester, S. C. De Smedt, *Nano Lett.* **2010**, *10*, 4435.
[19] S. K. Lai, J. Hanes, *Methods Mol. Biol.* **2008**, *434*, 81.
[20] K. Boeneman, B. C. Mei, A. M. Dennis, G. Bao, J. R. Deschamps, H. Mattoussi, I. L. Medintz, *J. Am. Chem. Soc.* **2009**, *131*, 3828.
[21] M. Dahan, S. Lévi, C. Luccardini, P. Rostaing, B. Riveau, A. Triller, *Science* **2003**, *302*, 442.
[22] J.-H. Kim, S. Lee, K. Park, H. Y. Nam, S. Y. Jang, I. Youn, K. Kim, H. Jeon, R.-W. Park, I.-S. Kim, K. Choi, I. C. Kwon, *Angew. Chem. Int. Ed. Engl.* **2007**, *46*, 5779.
[23] I. Koyama-Honda, K. Ritchie, T. Fujiwara, R. Iino, H. Murakoshi, R. S. Kasai, A. Kusumi, *Biophys. J.* **2005**, *88*, 2126.
[24] D. Vercauteren, H. Deschout, K. Remaut, J. F. J. Engbersen, A. T. Jones, J. Demeester, S. C. De Smedt, K. Braeckmans, *ACS Nano* **2011**, *5*, 7874.
[25] C. Kural, H. Kim, S. Syed, G. Goshima, V. I. Gelfand, P. R. Selvin, *Science* **2005**, *308*, 1469.
[26] T. Ragan, H. Huang, P. So, E. Gratton, *J. Fluoresc.* **2006**, *16*, 325.
[27] L. Quan, S. Liu, T. Sun, X. Guan, W. Lin, Z. Xie, Y. Huang, Y. Wang, X. Jing, *ACS Appl. Mater. Interfaces* **2014**, *6,*16166.
[28] S.-T. Yang, L. Cao, P. G. Luo, F. Lu, X. Wang, H. Wang, M. J. Meziani, Y. Liu, G. Qi, Y.-P. Sun, *J. Am. Chem. Soc.* **2009**, *131*, 11308.
[29] E. Genin, Z. Gao, J. A. Varela, J. Daniel, T. Bsaibess, I. Gosse, L. Groc, L. Cognet, M. Blanchard-Desce, *Adv. Mater.* **2014**, *26*, 2258.
[30] K. Welsher, Z. Liu, S. P. Sherlock, J. T. Robinson, Z. Chen, D. Daranciang, H. Dai, *Nat. Nanotechnol.* **2009**, *4*, 773.
[31] I. Izeddin, J. Boulanger, V. Racine, C. G. Specht, A. Kechkar, D. Nair, A. Triller, D. Choquet, M. Dahan, J. B. Sibarita, *Opt. Exp.* **2012**, *20*, 2081.
[32] A. Kechkar, D. Nair, M. Heilemann, D. Choquet, J.-B. Sibarita, *PLoS One* **2013**, *8*, e62918.

Received: June 24, 2014
Revised: September 23, 2014
Published online: December 15, 2014